Charge Density in Crystalline Arsenic†

STUART GOLIN AND J. A. STOCCO
University of Pittsburgh, Pittsburgh, Pennsylvania 15213
(Received 14 July 1969)

The charge density in crystalline arsenic is calculated from orthogonalized-plane-wave wave functions and compared with the covalent-bond models due to Pauling and to Cohen, Falicov, and Golin. There is good qualitative agreement; arsenic clearly has covalent features.

INTRODUCTION

THERE are several theories of the covalent bond,[1,2] including a discussion of the semimetals and related compounds comparing the band and bond viewpoints.[3]

The atomic structure of arsenic, $(4s^2)(4p^3)$, gives us a clue to its crystal structure. As the s electrons lie some 6 eV below the p electrons, we expect the latter to be dominant in binding. Thus, we might expect the three mutually perpendicular p orbitals to form a simple cubic (SC) structure. But this would require each p electron to be covalently bonded with *two* others on either side of the atom, which is energetically unfavorable. Further, according to Pauling, the bond strengths can be increased by s-p hybridization. This changes the bond angle and distorts the crystal from SC. The Pauling model provides relationships between the binding energy and bond angles in the crystal, and the excitation energy in the atom.

Cohen, Falicov, and Golin[3] (CFG) have calculated the band structure of As assuming a SC crystal and found this structure unstable; in the actual crystal structure of As, these instabilities disappear. They have also determined the approximate atomic and bonding character of many crystal wave functions at points of high symmetry in the Brillouin zone (BZ).

The crystal structure[3-6] of As is in fact close to SC, and can be obtained from it by applying two small and independent distortions: a shear and an internal displacement of atoms. The shear and the displacement are along the same body diagonal of the initial unit cube; this diagonal retains its threefold symmetry and is called the trigonal axis. In the resulting arsenic ($A7$) structure, two atoms are associated with each lattice point, and each atom has three nearest and three next-nearest neighbors. The crystal structure is illustrated in Fig. 1.

In this paper, we have calculated the charge density of crystalline arsenic, $\rho(\mathbf{r})$. The calculation illustrates the covalent nature of As, a semimetal, and confirms many qualitative ideas of Pauling[1] and CFG.[3] Also, we have estimated the "bonding charge," the charge transferred to the bond from the two bonding atoms. This charge is important in Phillips's[2] theory but is too small in As to make an appreciable contribution to the binding energy.

The Fourier coefficients of the charge density (or potential) are also very important in describing covalent bonds,[2] and these have already been calculated for As.[7] One of these coefficients, $F(\bar{1}11)$, differs appreciably from a superposition of atomic charge. Unfortunately, it is difficult to confirm the magnitude of this coefficient from x-ray measurements.[8]

The calculations of this paper are based on the results of a self-consistent orthogonalized-plane-wave (OPW) calculation,[7] referred to here as I. Both the plane wave and core parts of the wave functions were used.

In I, in the process of making the crystal potential self-consistent, the equivalent of 64 points (actually 13 different points) in the BZ were sampled using the Cohen and Keffer[9] technique. To test convergence, one can sample the equivalent of only 1 (Γ) or 8 (Γ,T,X,L) points. Here, Γ is the center of BZ, T is on the trigonal axis at the center of the regular hexagonal face, and L and X are the centers of the other hexagonal faces and of the rectangular faces, respectively. There are three equivalent L and X points, but only one Γ point and one T point. Further details of the crystal structure, BZ, and group theory are given in Refs. 4–7.

The room-temperature crystal-structure parameters[5] were used here and in I as the low-temperature parameters[6] have just recently been measured.

Atomic units are used throughout: 1 a.u. (energy) $=27.2$ eV; 1 a.u. (charge density) $=1.08\times10^{-6}$ C/cm^3; $\rho\equiv|\psi|^2$ is positive for electrons.

RESULTS

In calculating the charge density, we can average over the occupied levels at the equivalent of 1, 8, or 64 points in the BZ. The charge density so averaged is plotted along a nearest-neighbor direction in Fig. 2.

† Research supported in part by the Air Force Office of Scientific Research, Office of Aerospace Research, U. S. Air Force, under AFOSR Grant No. 196-66.

[1] L. Pauling, *The Nature of the Chemical Bond* (Cornell University Press, Ithaca, N. Y., 1960), 3rd ed.

[2] J. C. Phillips, Phys. Rev. **166**, 832 (1968); **168**, 905 (1968); **168**, 912 (1968); **168**, 917 (1968); and references cited therein.

[3] M. H. Cohen, L. M. Falicov, and S. Golin, IBM J. Res. Develop. **8**, 215 (1964); referred to as CFG.

[4] L. M. Falicov and S. Golin, Phys. Rev. **137**, A871 (1965).

[5] R. W. G. Wyckoff, *Crystal Structures* (Wiley-Interscience, Inc., New York, 1963), Vol. I.

[6] D. Schiferl and C. S. Barrett, J. Appl. Cryst. **2**, Pt. 1, 30 (1969).

[7] S. Golin, Phys. Rev. **140**, A993 (1965); referred to as I.

[8] C. S. Barrett (private communication).

[9] M. H. Cohen and F. Keffer, Phys. Rev. **99**, 1128 (1955).

TABLE I. Valence charge density at **O** and **M** averaged over 1, 8, and 64 points in the BZ. For comparison, values based on atomic models[a] are given.

	Nucleus (**O**)	Midpoint (**M**)
# points 1	36.0 a.u.	0.101 a.u.
8	31.3	0.081
64	31.9	0.073
ρ_{at}	24.9	0.058
ρ_{CFG}	33.6	0.068
ρ_P	...	0.073

[a] See Discussion section in text.

We see that 1 point in the BZ gives us a poor representation of the charge density, but that 8 and 64 points give densities differing at most by 10%. This leads us to believe that with 64 points, the charge density has converged to a few percent; and with only 8 points, it is probably good to 10 or 15%. (Plots along the second-nearest-neighbor direction lead to similar conclusions.)

Table I gives the charge density at the origin (nucleus), **O**, and at the midpoint between nearest neighbors, **M**. Again it is averaged over 1, 8, and 64 points.

The contour maps in Fig. 3 clearly demonstrate the covalent nature of As. We see an appreciable buildup of charge between first nearest neighbors but almost none between second nearest neighbors. (They are equivalent in the SC structure.) In plotting these maps, we averaged ρ over only 8 points in the BZ because of the prohibitive computer time required for 64 points.

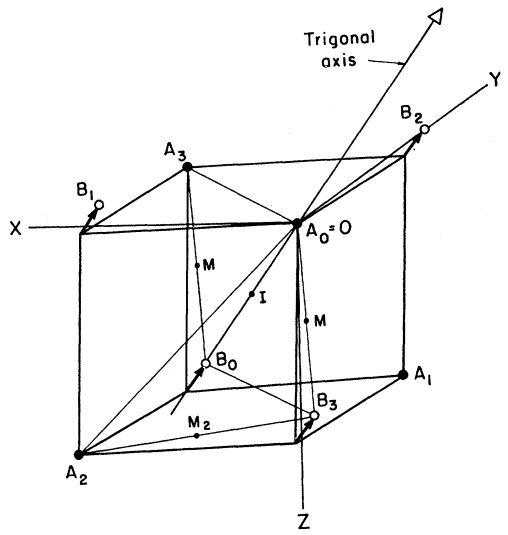

FIG. 1. Crystal structure of As showing similarity to SC structure. The internal displacement, indicated by arrows, splits the crystal into two sublattices, designated A and B. The nearest neighbors of A_0 and B_0 are B_1, B_2, B_3 and A_1, A_2, A_3, respectively. The translation vectors of As go from A_0 to A_1, A_2, and A_3. The origin, $A_0=\mathbf{O}$, is not an inversion center. **M** and $\mathbf{M}_2$ are midpoints between nearest and next-nearest neighbors, respectively; they are inversion centers. I, the midpoint between A_0 and B_0, has the full point group of the crystal and is often taken as the origin, as in Refs. 4 and 7. The vector from I to B_0 is called τ there. (X, Y, Z are rectangular axes.)

TABLE II. Charge density of the high symmetry levels[a] at **O** and **M**.

Level	**O**	**M**	Character[b]
Γ_1	10.0	0.015	s; B
Γ_2'	25.8	0	s; A
Γ_1	0.2	0.016	p; B
Γ_3	0	0.035	p; B
Γ_2'	4.4	0.[illegible]	p; A
Γ_3'	0	0	p; A
T_2'	14.1	0.023	B
T_1	7.7	0	A
T_3'	0	0.038	p; B
T_1	12.1	0	A
T_3	0	0	p; A
T_2'	7.5	0.000	B
X_4	16.0	0.028	s; A,B
X_1	9.5	0.063	p; B,A
X_1	7.0	0.000	s; B,A
X_4	0.2	0.012	p; A,B
X_3	0	0.034	p; A,B
X_1	0.5	0.001	d; B,A
L_1	11.1	0.029	A,B
L_4	12.1	0.038	B,A
L_4	1.3	0.033	B,A
L_2	0	0.046	p; A,B
L_1	3.2	0.006	A,B
L_4	9.7	0.012	B,A
L_1	2.9	0.008	A,B
L_3	0	0	p; A,A

[a] At each symmetry point, the levels are in ascending order of energy The ordering is from I except where contradicted by Ref. 13. The spacing indicates the position of the Fermi energy.
[b] Γ and X are from Ref. 3.

Table II presents information about individual energy levels at the points of highest symmetry: Γ, T, X, L. It gives the charge density at **O** and **M**, and gives the approximate character[3] of the level, s or p, and bonding (B) or antibonding (A). These assignments are based on group theory and on the nearness of As to SC. In some cases, no *a priori* assignment is possible—or meaningful.

The bonding character of an X level is complicated by the fact that there are three equivalent X points in the BZ and three midpoints (**M**) associated with each atom. Thus the wave function associated with a particular X point will have one behavior at one of the midpoints and a different behavior at the other two. For instance, a particular X_4 level will be antibonding $[\rho(\mathbf{M})=0]$ at *one* midpoint and bonding [at least $\rho(\mathbf{M})\neq 0$] at the other *two*. This is indicated by placing the A *before* the B in the appropriate column in Table II. The tabulated charge density refers, of course, to the midpoint at which the wave function is bonding. The same applies to L.

The normalization in Table II is such that each level holds 2 electrons per primitive cell, or one electron per atom. Then each level corresponds to one atomic orbital. For the doubly degenerate levels (Γ_3,Γ_3',T_3,T_3'), the numbers refer to just one of the levels.

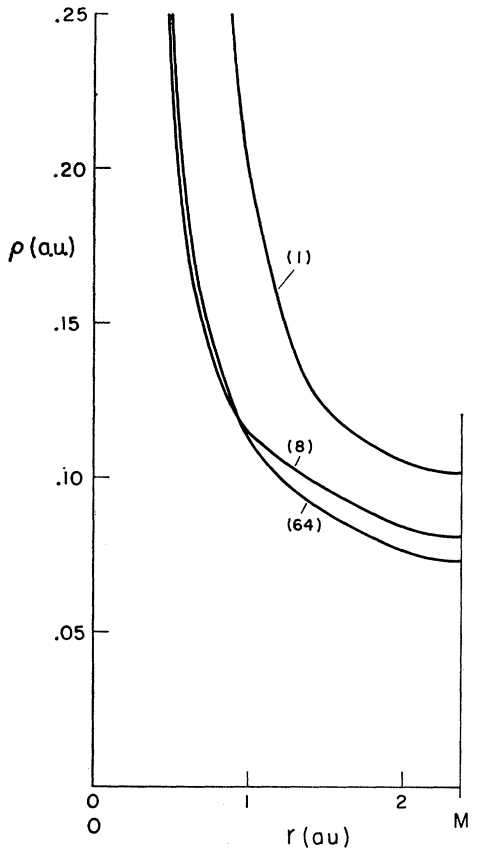

FIG. 2. Charge density averaged over the equivalent of 1, 8, and 64 points in the BZ is plotted along a nearest-neighbor direction.

DISCUSSION

A. CFG Model

In the simplest atomic description of the As band structure, the bands are (in increasing energy): bonding s, antibonding s, 3 bonding p, 3 antibonding p. The Fermi energy (E_F) should be between the bonding p and antibonding p bands. This picture holds well at Γ, where hybridization effects are minimal, as we see in Table II. While the levels at T, X, and L are not this simple, there is a tendency for most of the charge at **O** to come from the lower-lying levels, and for the levels above E_F to be antibonding or weakly bonding.

In interpreting the numbers in Table II, we compare them with free-atom values based on Hartree-Fock (HF) wave functions.[10] Then for a $4s$ orbital in a free atom, $\rho_{4s}(0)=\frac{1}{2}\rho_{at}(\mathbf{O})=12.4$ a.u. (Table I). Thus, if for some crystal level $\rho(\mathbf{O})\ll 12.4$ a.u., we can conclude that the level has little s character (since each band corresponds to one atomic orbital).

Hybridization between s and p (and d) orbitals occurs for most of the levels; only in a few cases where symmetry requires $\rho(\mathbf{O})=0$ can we exclude s character. Yet the atomic designations of CFG work well at Γ and reasonably well at X (except for the lowest X_1 level). Hybridization is very strong at T and L, and perhaps the best way to assign atomic character would be based on the calculated charge density at the nucleus.

A measure of the degree of bonding is provided by $\rho_{at}(\mathbf{M})$, which is a superposition of free-atom charge densities at **M** (see Table I). Since the $4s$ and $4p$ orbitals in As have a similar radial dependence and magnitude far from the nucleus, we can divide this charge equally among the five orbitals: $\rho_{\rm orb}(M)\cong\frac{1}{5}\rho_{at}(\mathbf{M})=0.012$ a.u. Thus, if for some crystal level $\rho(\mathbf{M})>0.012$ a.u., the level may be considered bonding; for the antibonding levels $\rho(\mathbf{M})=0$. In between, the levels are nonbonding or weakly bonding.

The bonding and antibonding designations are seen in Table II to hold well for most of the levels. As already noted, at X and L, a level may be bonding at one midpoint and antibonding at two others, or vice versa. This complicates a chemical interpretation of these levels, but poses no problems with a band view.

We can use the model to calculate the total charge density at **O** and **M**, $\rho_{\rm CFG}(\mathbf{O})$ and $\rho_{\rm CFG}(\mathbf{M})$. From free-atom wave functions,[10] we form Bloch functions transforming according to $\mathbf{k}=\mathbf{O}(\Gamma)$ which are bonding s, antibonding s, and bonding p. In normalizing these functions, we allow for the appreciable overlap between nearest neighbors: $(4s,4s)=0.17$ and $(4p,4p)=0.35$ for p orbitals directed along the line of centers. The results are given in Table I; compared with the detailed calculation, they are accurate to about 7%. The errors in the nonbonding atomic calculation of ρ_{at} are about three times larger.

B. Pauling Model

According to Pauling,[1] the strength of the covalent bond is increased if the $4s^24p^3$ configuration is hybridized with one or more excited states. The lowest-lying excited state[11] $4s^24p^25s$ has an excitation energy $\Delta=0.24$ a.u. At slightly higher energies are[11] $4s4p^4$ and $4s^24p^24d$. The $4p^3$ configuration has bonds at right angles (SC), and the three excited states mentioned lead to planar bonds making angles of 120° with each other. Experimentally, the bond angle is[5] 97.3°, so that hybridization is small. Thus, it is probably not too important which excited state one chooses, and we have based our calculations on the lowest one, $4p^25s$, as it is the simplest to work with. (This is actually a poor choice as the $5s$ orbital has a node near **M**, making it ineffective in bonding; but most of the results apply also to the $4s4p^4$ configuration.) Following Pauling we write

$$\text{configuration}=\alpha(sp^2)+\beta(p^3)$$

and assume that the radial parts of the two configura-

[10] R. E. Watson and A. J. Freeman, Phys. Rev. **124**, 1117 (1961).

[11] C. E. Moore, *Atomic Energy Levels*, Natl. Bur. Std. (U. S.) Circ. No. 467 (U. S. Government Printing Office, Washington, D. C., 1952), Vol. II.

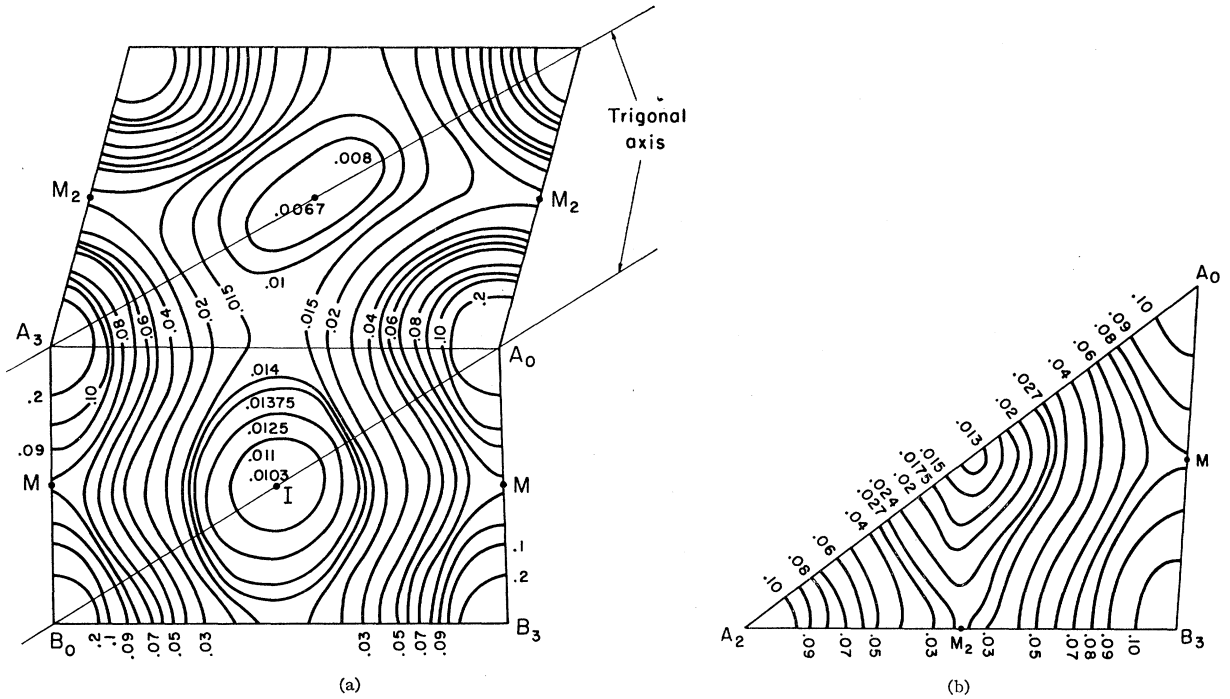

(a) (b)

FIG. 3. Contour maps. Notation refers to Fig. 1. (a) Map in a mirror plane; (b) another plane.

tions are the same (poor for the 5*s* orbital). From the experimental value of the bond angle, we find $\alpha=0.20$, which justifies our assertion that the hydridization is small. We can now estimate the binding energy[1]: $\mathrm{BE}\cong 3\alpha\Delta/(1-\alpha)=0.18$ a.u., about 60% above the experimental value[12] of 0.11 a.u.

The model allows us to calculate the charge density at **M**, $\rho_P(\mathbf{M})$. We find that hybridization increases the bonding *p* charge density at **M** by the factor $[(1-\frac{1}{3}\alpha^2)^{1/2}+\frac{1}{3}\alpha]^2=1.13$. This does not allow for the change in normalization resulting in the increase in overlap of the wave functions caused by the hybridization. We expect the overlap to increase by about this factor of (1.13) to 0.39. We treat the $4s^2$ electrons as in the CFG model. The resulting charge density agrees with the detailed OPW result (see Table I); the agreement is certainly better than the approximations and uncertainties in both calculations, and must be considered fortuitous.

C. Valence Charge Density at Nucleus

The various parts of the Fermi surface of As[3,4,7,13] are at *L* and near *T*. From Table II, we see that the charge density at the nucleus from states near the Fermi surface is larger than one might expect on a simple chemical picture, as the *p* electrons are dominant in bonding. These numbers should be useful in interpreting Knight shift measurements.

The total valence charge density at the nucleus averaged over 64 points in the BZ, $\rho(\mathbf{O})$ (Table I), should be useful in interpreting isomer-shift[14] measurements. $\rho(\mathbf{O})$ is about 30% higher than the free-atom value, and this difference appears to be much larger than any convergence error. At first it might seem that this implies hybridization: a 4*p* electron is excited into a 5*s* state. But this, in fact, would make a contribution to $\rho(\mathbf{O})$ two orders of magnitude less than the observed difference. This is because the admixture of the 5*s* state is small, 0.2 at most, and because $\rho_{5s}(\mathbf{O})$ is small: we have calculated it to be 0.93 a.u. (in the Hartree approximation).

The increase in $\rho(\mathbf{O})$ can be easily accounted for as a normalization effect. In calculating $\rho_{\mathrm{CFG}}(\mathbf{O})$ for Table I, we calculated $\rho(\mathbf{O})$ for bonding *s* and antibonding *s* orbitals, and found separate contributions of 8.3 and 25.1 a.u., respectively. Note that the latter is about twice the free-atom value. The difference is due entirely to different normalization factors:

$$[1\pm 3(4s,4s)]^{-1/2}(+,\ \text{bonding};\ -,\ \text{antibonding}).$$

Incidently, these values of $\rho(\mathbf{O})$ are very close to those for Γ_1 and Γ_2', respectively.

D. Bonding Charge and Binding Energy

The bonding charge, of interest in Phillips's[2] model, is the additional charge in the region between first

[12] C. Kittel, *Introduction to Solid State Physics* (John Wiley & Sons, Inc., New York, 1966), 3rd ed., p. 78.
[13] P. J. Lin and L. M. Falicov, Phys. Rev. **142**, 441 (1966).
[14] See, e.g., H. Frauenfelder, *The Mossbauer Effect* (W. A. Benjamin, Inc., New York, 1962).

nearest neighbors over that resulting from the superposition of atomic charge. We may define it by

$$Q=\int[\rho(\mathbf{r})-\rho_{at}(\mathbf{r})]\,d^3r,$$

where the integration is limited to the region about **M** in which the integrand is positive. We estimate $Q\approx 0.03$ a.u.

One can also estimate Q from the Fourier coefficients of the self-consistent potential calculated in *I*. One of these, $F(\bar{1}11)$, differs appreciably from the free-atom value and also leads to $Q\approx 0.03$ a.u. Thus, as anticipated in I, the bonding charge is largely represented by this Fourier coefficient.

According to Phillips,[2] the volume occupied by the bonding charges should be very small. We estimate the (total) volume occupied by the three bonding charges in the primitive cell to be about 4% of the volume of that cell.

The ionic binding energy per atom from this charge is ≈ 0.002 a.u., negligible compared with the experimental value of 0.11 a.u. Actually, on an atomic picture, most of the binding energy comes simply from the (nonbonding) overlap of the spherical charge distributions of nearest neighbors. Using HF wave functions,[10] we have calculated this energy to be 0.30 a.u.; thus, the repulsive terms must contribute at least -0.2 a.u. to the binding energy.

ACKNOWLEDGMENTS

We wish to thank C. S. Barrett, M. H. Cohen, L. M. Falicov, W. Goldburg, D. Haftmeister, F. Keffer, I. Lowe, D. Schiferl, and P. Stone for useful conversations.

PHYSICAL REVIEW B VOLUME 1, NUMBER 2 15 JANUARY 1970

Resistivity of Iron as a Function of Magnetization and Stress*

P. W. Shumate, Jr.,† R. V. Coleman, and R. C. Fivaz
Department of Physics, University of Virginia, Charlottesville, Virginia 22903
(Received 2 June 1969; revised manuscript received 6 October 1969)

The resistance and magnetoresistance of iron single crystals have been measured as a function of stress at liquid-helium temperatures. For measuring currents above some critical value, a large transition in the resistance of the sample is observed, and the critical current for this transition is a function of both the applied longitudinal magnetic field and the applied axial stress. The results have been interpreted in terms of inverse-magnetostriction and domain-reorientation effects involving the self-field of the current. We have developed a model for the ⟨100⟩-axial crystals based on a sheath-core configuration with spins perpendicular and parallel to the current in the sheath and core, respectively. Under favorable conditions the formation of the sheath-core configuration simulates the behavior of thermodynamical variables in a first-order phase transition. The analysis of the model can be used to predict the observed resistance transition quite accurately and can also be used to obtain a value of the saturation magnetostriction constant λ_{100}. The value obtained is $\lambda_{100}=(25.0\pm1.0)\times10^{-6}$, which is in reasonable agreement with other measurements. Results of stress experiments on ⟨111⟩-axial crystals are consistent with a negative value of λ_{111}, but indicate that the field and current-induced resistance transitions are more complex than those in the ⟨100⟩-axial crystals. Discussion of possible mechanisms is included.

I. INTRODUCTION

In previous papers,[1–3] we have reported results of electrical-resistance measurements in iron single crystals, particularly in the low-temperature range extending to 1°K. A striking characteristic has been large negative magnetoresistance behavior observed in the liquid-helium temperature range. In the case of ⟨100⟩ specimens, this behavior was shown to be primarily induced by the self-field of the measuring current and was interpreted as a reverse galvanomagnetic effect[3] connected with the formation of various domain configurations.

In this paper, we report on a series of results obtained by applying uniaxial stress to the crystal and measuring resistance as a function of stress, magnetic field, and measuring current. The use of uniaxial stress as an additional variable has allowed a precise control of the magnetic state of the crystal through inverse magnetostriction. This has allowed us to make a more complete interpretation of the resistance and magnetoresistance behavior in the helium temperature range, and has also provided a fairly accurate value of the magnetostriction constant for iron at helium temperatures.

* Work supported in part by the U. S. Atomic Energy Commission and the U. S. Army Research Office, Durham, N. C.
† Present address: Bell Telephone Laboratories, Murray Hill, N. J.
[1] A. Isin and R. V. Coleman, Phys. Rev. **142**, 372 (1966).
[2] R. V. Coleman and A. Isin, J. Appl. Phys. **37**, 1028 (1966).
[3] G. R. Taylor, A. Isin, and R. V. Coleman, Phys. Rev. **165**, 621 (1968).